

RESEARCH ARTICLE

Modeling and Interpretation of Geothermal System Components Using the Gravity Method at the “X” Geothermal

Mochammad Malik Ibrahim^{1,*}, Pri Utami², Imam Baru Raharjo³

¹ Department of Geological Engineering, Sriwijaya University, Palembang, Indonesia

² Department of Geological Engineering, Gadjah Mada University, Yogyakarta, Indonesia

³ PT. Pertamina Geothermal Energy, Indonesia

* Corresponding author : malikibrahim100@ft.unsri.ac.id
Tel.:+62-856-4256-2626
Received: Jun 1, 2023; Accepted: May 22, 2024.
DOI: 10.25299/jgeet.2024.9.2.13032

Abstract

Geothermal field "X" is one of the geothermal fields located in North Sulawesi Province managed by PT Pertamina Geothermal Energy. This research aims to determine the presence of geothermal system components in the subsurface using the gravity method. Gravity method data processing is processed with observational and theoretical corrections to obtain a complete Bouguer anomaly. The complete Bouguer anomaly is separated into regional and residual anomaly using the upward continuation process. The results of modeling and interpretation of residual (shallow) gravity prove the existence of 3 (three) rock layers and their density values, Post Tondano Andesite Unit layer (2,4 g/cm³), Tondano Rhyolite Unit layer (2,5 g/cm³) and Pre Tondano Andesite Unit layer (2,7 g/cm³). The results of modeling and interpretation of regional (deep) gravity evidence the existence of 3 (three) rock layers along with the rock density value, Tondano Rhyolite Unit layer (2,5 g/cm³), Pre Tondano Andesite Unit layer (2,7 g/cm³) and diorite intrusion rock layer (2,9 g/cm³). The geothermal system in the research area is composed of Post Tondano Andesite Unit as overburden rock, Tondano Rhyolite Unit as caprock, Pre Tondano Andesite Unit as reservoir rock and Diorite intrusion rock as heat source.

Keywords: Geothermal field "X", gravity method, complete Bouguer anomaly, gravity modeling, geothermal system components

1. Introduction

The "X" geothermal field is geographically located in the eastern part of Indonesia (north arm of Sulawesi Island) and is located \pm 30 km south of the city of Manado, North Sulawesi Province (Figure 1). This area is located in a volcanic area with a very large caldera, namely the Tondano caldera. This area is in a row of volcanoes (V. Lengkoan, V. Kasuratan and V. Tampusu) and a crater lake known as Lake Linau. This area is at an altitude of 750 m to 1200 m above sea level (Ibrahim et al, 2022).

The geothermal system in the research area is still affected by volcanic and tectonic activity in the Sangihe Arc to this day. The heat source is thought became a breakthrough of igneous rock which is still actively transferring heat to the environment in the area around Lake Linau. Geothermal manifestations found around Lake Linau consist of active and inactive geothermal manifestations. The presence of geothermal manifestations on the surface indicates the existence of a component of the geothermal system below the earth's surface (Utami, 2011).

Geothermal Exploration "X" began in 1973, since the first commercial operation in 2001 with a capacity of 1 x 20 MWe. At present the field continues to grow until it reaches 6 x 20 MWe (Fanani et al, 2021) with an area of around 14 Km² and has a total of 46 installed wells (Utami et al, 2021). According to Lestari & Sarkowi (2013) in a research using second vertical derivative (SVD) gravity anomaly data, it was shown that the results of the analysis of fault and fault structures led to the formation of Lake Tondano as part of the geothermal system controller in the research area.

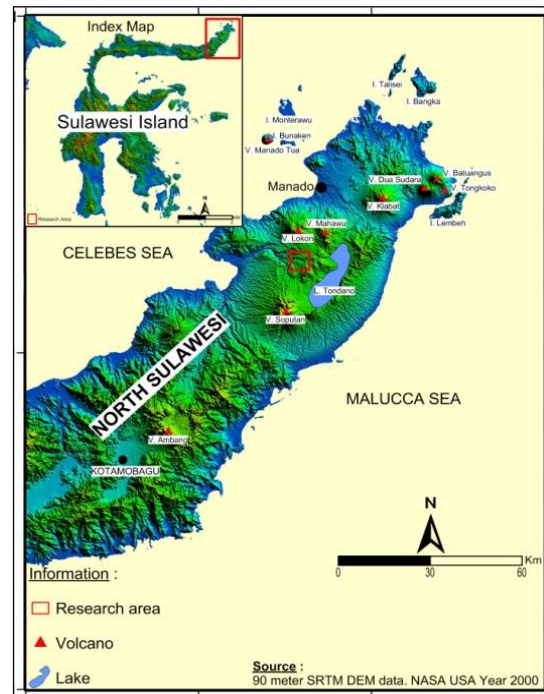


Fig 1. Map of research locations (modification from Ibrahim et al, 2022)

This research aims to interpret geothermal system components such as cap rock, reservoir rock, fracture and heat source based on subsurface gravity modeling in the research area.

2. Geology of the Research Area

The geological conditions of the research area are dominated by tertiary (Miocene) volcanic rocks which are formed as bedrock composed of thick layers of hyaloclastites and lava flows with inserts of sedimentary formations. During the late Miocene or early Pleistocene there was a major eruption forming the large Lake Tondano caldera which was produced by volcano tectonic depression, characterized by very wide expanses of tuff rock.

A regression and acceleration of volcanic activity in North Sulawesi caused to the Tondano explosion, followed by the

Pliocene/Pleistocene Pangolombian eruption. The two calderas still dominate the topography today and are modified by Lake Linau and Lake Tondano (Brehme et al, 2014).

Several eruption centers formed inside and margins of the Tondano depression, one of which formed the small Pangolombian depression. Geology in detail has been described by the Pertamina Upstream Technology Center (2013) and Utami, et al (2015) shown in Figure 2. This system is formed by volcanic rocks in steep areas. The rocks include andesitic and pyroclastic lava from the Pangolombian, Kasuratan, Lengkoan, Tampusu and Linau eruption centers.

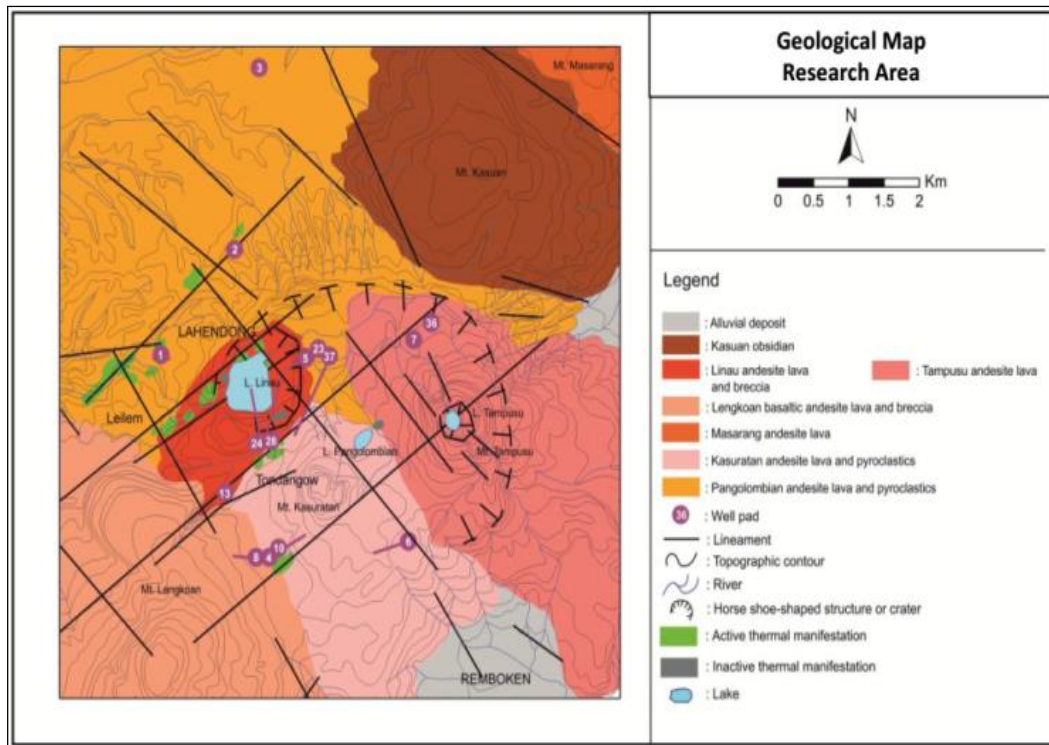


Fig 2. Geological map of the research area (modification from PT. Pertamina UTC, 2013, Utami et al, 2015)

The geological section profile (Figure 3) of the research area is based on the integration of subsurface rock unit data, current measured temperature, well configuration and geological structure results. From the oldest to the youngest rocks starting from Pre-Tondano Andesite Unit, Tondano Rhyolite Unit and Post-Tondano Andesite Unit. Pre-Tondano Andesite Unit and Tondano Rhyolite Unit were intruded by dyke diorite (Utami, 2011).

This geothermal manifestation is dominated by the emersion activity of acidic steam-heated hot fluids, which produce hydrothermal alteration rocks. Geothermal manifestations are in the form of hot springs and hot pools with neutral pH and temperatures reaching 70⁰ - 90⁰ C which are partly associated with fumaroles, steaming ground (T = 60⁰ - 95⁰ C) with a depth of 15 cm, mudpots, mudpools and mudpond (Sidqi & Utami , 2018).

Fault zone appears to be a vertical boundary separating a northern area with acidic brine, considerable gas discharge, high productivity, and strongly altered rocks from a southern section hosting neutral water, higher temperatures, and less altered rocks. The fluid flow and geochemical reactions

were found to be mainly controlled by the permeability in fault-related fractures (Brehme et al, 2016).

Volcanic activity after the formation of the caldera begins with lava and tuff of Mount Lengkoan. Subsequent activities include the deposition of andesitic lava and tuff of Mount Kasuratan, andesite lava of Mount Tampusu, tuff and obsidian of Mount Kasuan, and lava and andesite breccia of Mount Linau. The andesitic lava and breccia of Mount Linau are known to be 0.458 ± 0.042 Ma or middle Pleistocene. The youngest volcanic activity precipitated breccia and andesitic lava from Mount Masarang, followed by colluvial deposits. The development of volcanism in the research area can be determined based on the character of the rocks and the volcanic stratigraphic sequence (Kristiawan et al, 2013).

Stratigraphy of the research area according to Utami (2011) was compiled based on the results of age dating analysis using the radioactive element K/Ar (Figure 4). The grouping of subsurface stratigraphic units in the research area is divided into 4 (four) rock units based on the age of the oldest to the youngest, namely: Pre-Tondano andesite Unit, Tondano Riolite Unit, Post-Tondano Unit and Diorite.

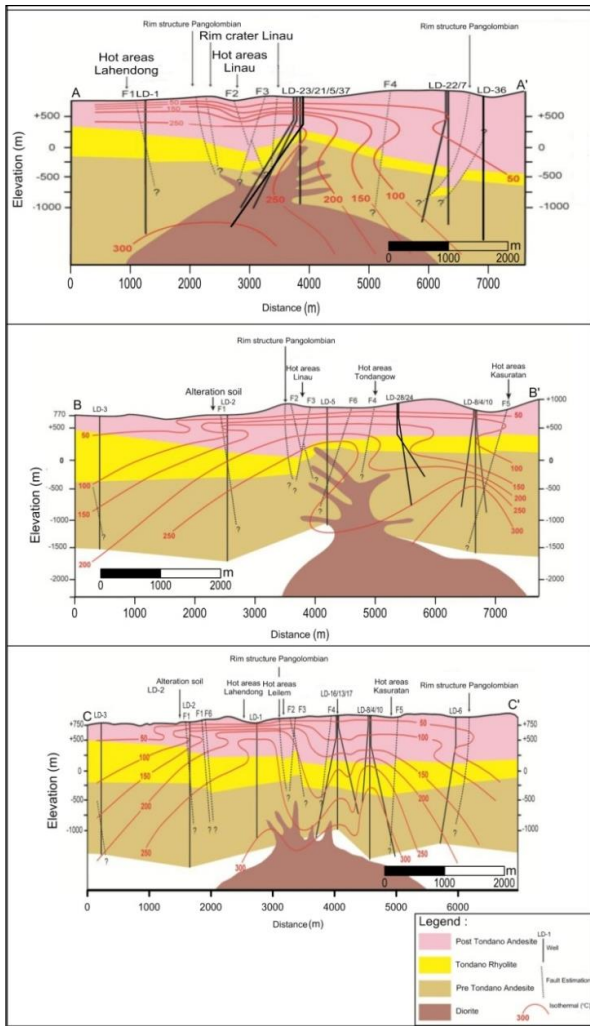


Fig 3. Geological cross section (modification from Utami, 2011; PT. Pertamina UTC, 2013)

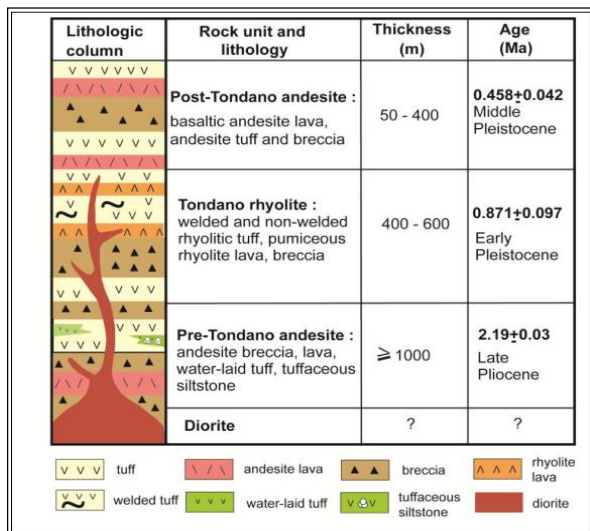


Fig 4. Stratigraphic column of the research area (Utami, 2011)

3. Gravity Method

The basic principle of the gravitational method is Newton's law of attraction between particles. Newton's law states that the attractive force between two particles with masses m_0 and m separated by a distance of $\vec{r}_2 - \vec{r}_1$ from the center of mass (Figure 5) is proportional to the multiplication of the mass m_0

by m and inversely by the square of the distance. This force is described in equation (1).

$$\vec{F}(\vec{r}) = -G \frac{m_1 m_2}{|\vec{r}_2 - \vec{r}_1|^2} \times \frac{(\vec{r}_2 - \vec{r}_1)}{|\vec{r}_2 - \vec{r}_1|} \quad (1)$$

where $\vec{F}(\vec{r})$ is the force acting on m due to m_0 and has a direction opposite to the direction $|\vec{r} - \vec{r}_0|$ [that is, from m_1 to m_2 , while G is the general constant of gravity which is $6.67428 \times 10^{-11} \text{ Nm}^2 \text{ kg}^{-2}$ or $\text{m}^3 \text{ kg}^{-1} \text{ s}^{-2}$.

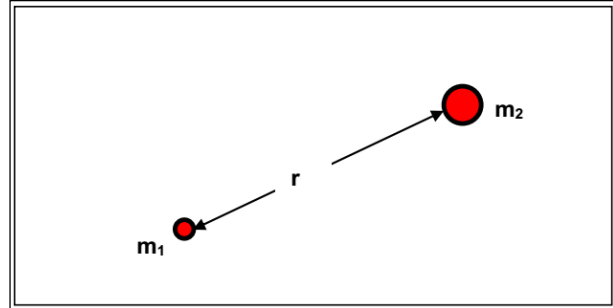


Fig 5. Attraction force (F) between two masses; m_1 and m_2 at distance r apart (Alsadi & Baban, 2014)

The gravity method is a geophysical method passive which is sensitive to acceleration variations Earth's gravity is caused by density differences rock (Dentith & Mudge, 2014).

3.1 Gravity Field Anomaly

Gravity anomaly is difference between the measured gravity and the theoretical gravity derived from a reference body, after some corrections (Balmino & Bonvalo, 2016).

Changes in the Earth's gravitational acceleration caused by local anomaly objects are called gravitational anomaly. This anomaly is denoted by Δg , when compared to the Earth's gravitational field it is very small ($\Delta g \ll g$). Gravity anomaly can only be measured with the Earth's gravitational field in the same direction (Gregg et al, 2010).

3.2 Gravity Data Reduction

The measurement value of gravity on the earth's surface depends on the mass distribution inside the earth and the shape of the earth itself, while the influencing factors are the centrifugal force due to the earth's rotation and the effect of the tides due to the position of the moon and sun. Gravity anomaly is the value of gravity caused by differences in density contrast values under the earth's surface. To obtain a gravity anomaly below the gravity measurement point, several corrections are needed, namely tidal correction, theoretical gravity, free air correction and topographic correction.

Gravity field anomaly is defined as the difference between the measured gravitational field values in the topography or position (x,y,z) with the theoretical gravitational field in the topography for the same location. This gravitational field anomaly is caused by the density contrast beneath the earth's surface. Measured gravity field anomaly together with the earth's gravitational field.

Theoretical gravitational field is a field that exists due to non-geological factors and its value is calculated based on the elaboration of the theoretical formula. This field value is influenced by latitude, altitude and topographic mass around the measuring point (Sumintadireja et al, 2000).

3.2 Gravity Data Source

The data source used in the gravity method is exploration gravity measurement data obtained from PT. Pertamina Geothermal Energy. Gravity measurement data comes from measurements of Scintrex Autograv CG-5 gravimeter, instrument height, tidal correction values, measurement time,

and position data (coordinates). The number of observation gravity measurement stations is 46 points with random distribution over a survey area of 5 x 5 km² (Figure 6).

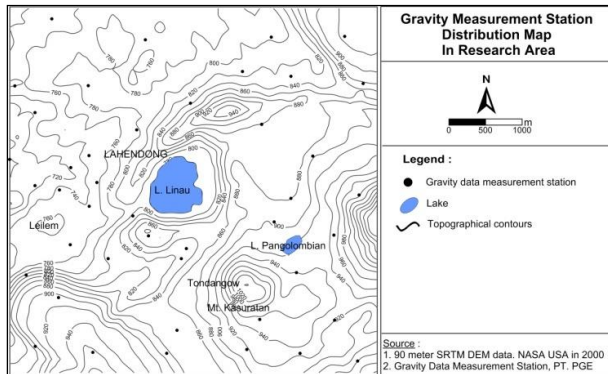


Fig 6. Map of the distribution of gravity measurement stations

4. Research Methodology

Gravity data obtained from PT. Pertamina Geothermal Energy in the form of data that has been processed from various kinds of observational corrections (tool height correction, tide correction, drift correction) and theoretical (latitude correction, free air correction, simple Bouguer correction, terrain correction). From the results of the observational and theoretical corrections, a complete Bouguer anomaly value is obtained.

4.1 Complete Bouguer Anomaly

The complete Bouguer anomaly is defined as the difference between the measured gravitational field values in the topography (x,y,z) and the theoretical gravitational fields in the topography (Sarkowi, 2014). The complete Bouguer anomaly is caused by the presence of density contrast beneath the earth's surface. LaFehr's (1991) statement can be expressed in the form of equation (2).

$$\Delta g_{obs}(x, y, z) = g_{obs}(x, y, z) - g_n(x, y, z) \quad (2)$$

where $\Delta g_{obs}(x, y, z)$ is the gravity field anomaly in topography, $g_{obs}(x, y, z)$ is the observed gravity field in topography and $g_n(x, y, z)$ is the theoretical gravity field in topography.

4.2 Upward Continuation

Continuation is the process of seeing an anomaly response from a field with a certain height (Telford et al, 1990). The upward continuation process is carried out using the Magpick software at a certain height according to the depth of the target anomaly.

4.3 Gravity Forward Modeling (GFM)

Gravity forward modelling comprises methods for the computation of the gravity field of some mass distribution, very often of the topography, but also from water, ice and crustal masses. GFM in the spatial and spectral domain are important for gravity applications in physical geodesy (e.g., gravity reduction, interpolation and prediction, e.g., for the construction of detailed gravity maps) and potential field or planetary geophysics (reduction and interpretation of gravity observations) (Hirt, 2015).

The modeling used in this research is forward modeling, which is a model resulting from an anomaly response model approach with field anomaly response data. This research conducts forward modeling to look the estimated response to gravity anomaly and targets in the form of geological structures and subsurface rock layers in geothermal areas.

Residual and regional anomaly maps are used as data became model by creating 3 (three) sections using Geosoft Oasis Montaj 6.4.2 menu software GM-SYS supported by geological map information and rock density variation values.

5. Results and Discussion

The complete Bouguer anomaly map (Figure 7) shows the distribution of anomaly values ranging from 3 to 16 mGal with high anomaly values in areas where active and inactive thermal manifestations occur stretching from west (W) to northwest (NW) and partly to the west (W) to the northwest (NW). east direction (E) research area. Meanwhile, the distribution of low anomaly values is in the south direction and a small part is in the northeast (NE) research area.

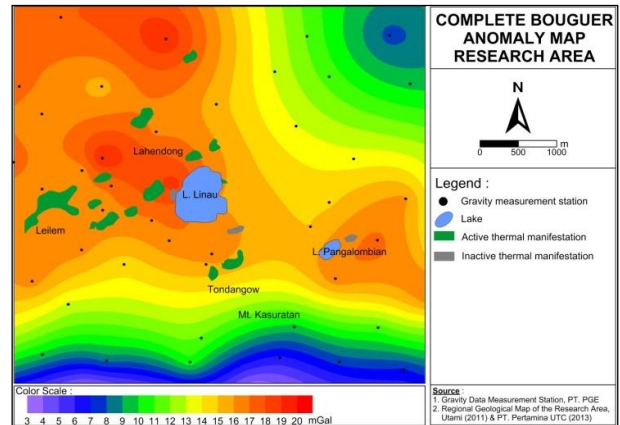


Fig 7. Complete Bouguer anomaly map

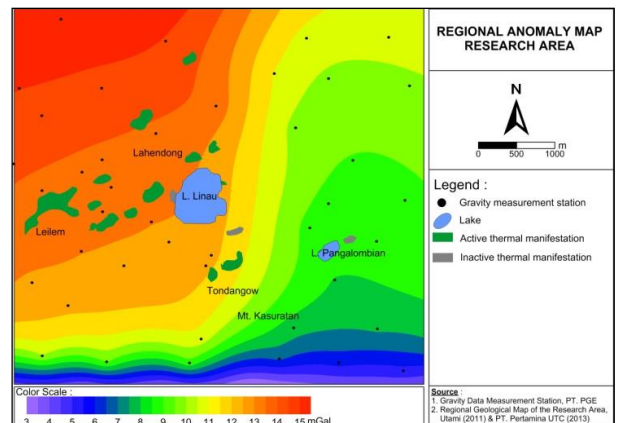


Fig 8. Regional anomaly map

The regional anomaly map (Figure 8) shows the distribution of the anomaly values obtained which range from 3 to 16 mGal with high values in the northwest (NW) direction and low values in the south (S) and northeast (NE) directions. This regional anomaly shows a smooth contour pattern because it can transform the measured potential field so that the measured potential field tends to accentuate anomaly caused by deep sources (regional effects) by eliminating anomaly caused by shallow sources (residual effects).

The residual anomaly map (Figure 9) shows the distribution of anomaly values having a range of -12 to 2 mGal with high anomaly values in the east (E) direction and some in the west - northwest direction (WNW). The distribution of low anomaly values is in the south (S) and northeast (NE) directions. This residual gravity anomaly is associated with shallow anomaly sources caused by the presence of geological structures and rock density variation values.

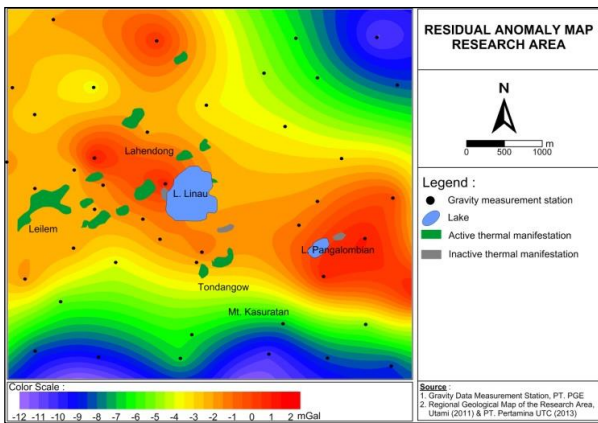


Fig 9. Residual anomaly map

5.1 Residual Anomaly Modeling and Subsurface Interpretation

The residual gravity anomaly map is strongly influenced by the presence of shallow anomaly sources caused by the presence of geological structures and rock density variation values in the research area. This residual gravity modeling aims to determine the value of rock density and a description of the shallow subsurface geological conditions.

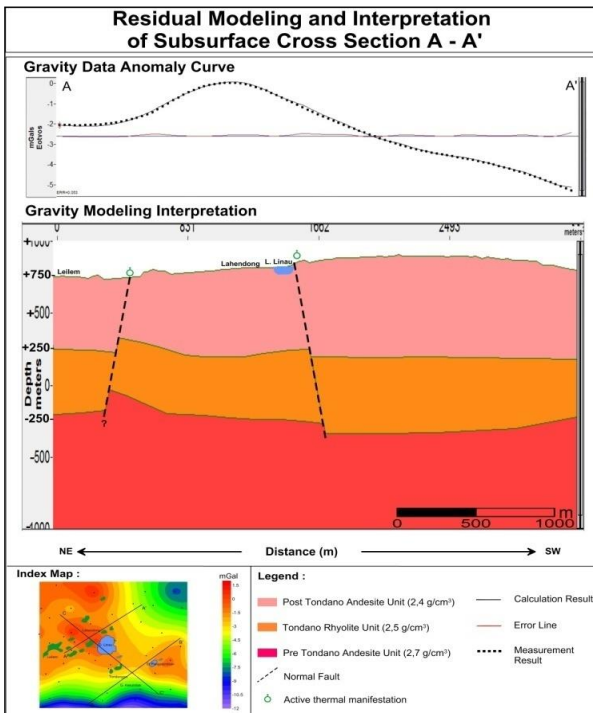


Fig 10. Residual modeling and interpretation of subsurface cross section A-A'

1) Cross Section A - A'

The results of residual gravity modeling cross sections A – A' (Figure 10) show shallow subsurface geological conditions with depths ranging from 750 m to (–1000) m. The results of modeling and interpretation of residual (shallow) gravity prove that there are 3 (three) rock layers along with rock density values, namely rock layers with density values (2,4 g/cm³) estimated became Post-Tondano Andesite Units, rock layers with density values (2,5 g/cm³) is estimated became the Tondano Rhyolite Unit and the rock layer with a density value (2,7 g/cm³) is estimated became the Pre-Tondano Andesite Unit. Based on geological information, it is known that there are 2

(two) normal structures in the Tondano Rhyolite Unit layer to the Post-Tondano Andesite Unit layer on the surface. The normal structure located in the SW direction of Lake Linau is interpreted to reach a depth of (–1000) m and to the NE side of Lake Linau is interpreted to reach a depth of (–200) m. This structure controls the presence of active thermal manifestations on the surface (upflow).

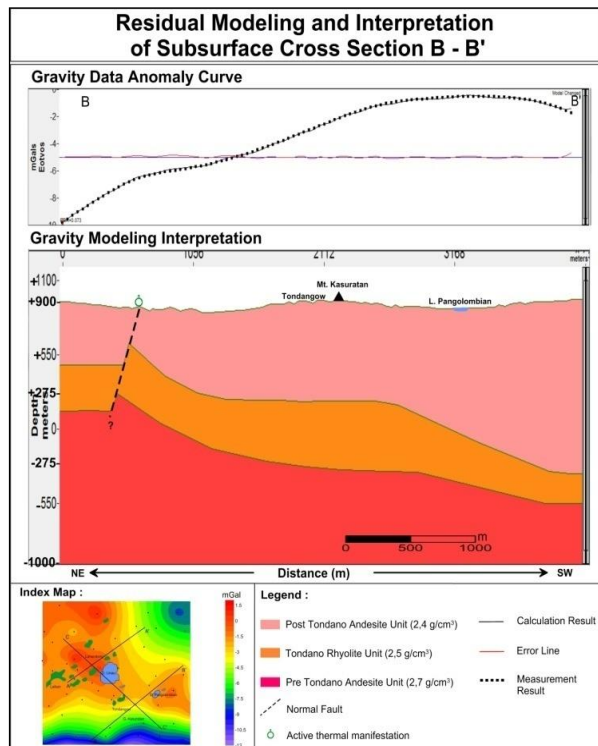


Fig 11. Residual modeling and interpretation of subsurface cross section B-B'

2) Cross Section B - B'

The results of residual gravity modeling cross section B – B' (Figure 11) show shallow subsurface geological conditions with depths ranging from 900 m to (–1000) m. The results of the modeling and interpretation of residual (shallow) gravity prove that there are 3 (three) rock layers along with the rock density values, namely rock layers with a density value of (2,4 g/cm³) estimated became the Post-Tondano Andesite Unit, rock layers with a density value of (2,5 g/cm³) is estimated became the Tondano Rhyolite Unit and the rock layer with a density value (2,7 g/cm³) is estimated became the Pre-Tondano Andesite Unit. The normal structure is located in the NE direction next to Tondangow Village which is interpreted to reach a depth of 150 m.

3) Cross Section C - C'

The results of residual gravity modeling cross section C – C' (Figure 12) show shallow subsurface geological conditions with depths ranging from 800 m to (–400) m. The results of the modeling and interpretation of residual (shallow) gravity prove that there are 3 (three) rock layers along with the rock density values, namely rock layers with a density value of (2,4 g/cm³) estimated became the Post-Tondano Andesite Unit, rock layers with a density value of (2,5 g/cm³) is estimated became the Tondano Rhyolite Unit and the rock layer with a density value (2,7 g/cm³) is estimated became the Pre-Tondano Andesite Unit. The normal structures located in the NW and SE directions next to Lake Linau are interpreted to reach depths of (-150) m and (–300) m, respectively.

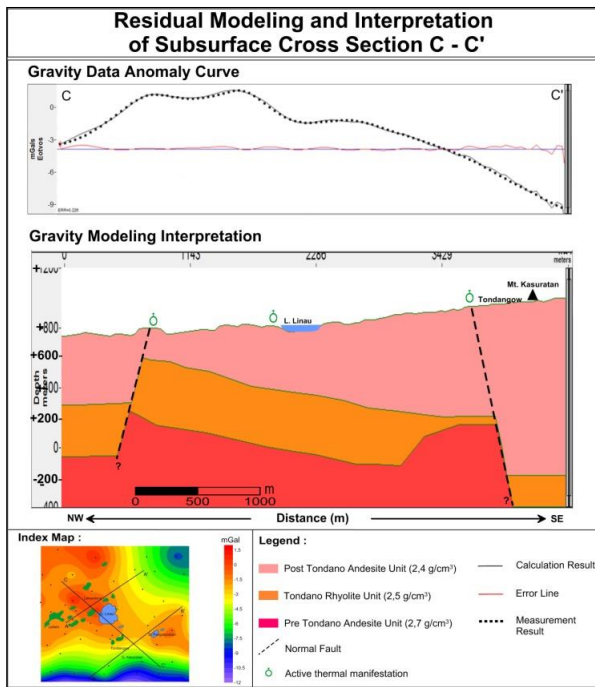


Fig 12. Residual modeling and interpretation of subsurface cross section C-C'

5.2 Regional Anomaly Modeling and Subsurface Interpretation

The regional gravity anomaly map is strongly influenced by deep anomaly sources caused by rock intrusion in the research area. This is reflected by contours with high values, while contours with lower values are caused by the presence of subsurface rock with lower density. This regional gravity modeling aims to determine rock density values and describe the geological conditions beneath the deep surface.

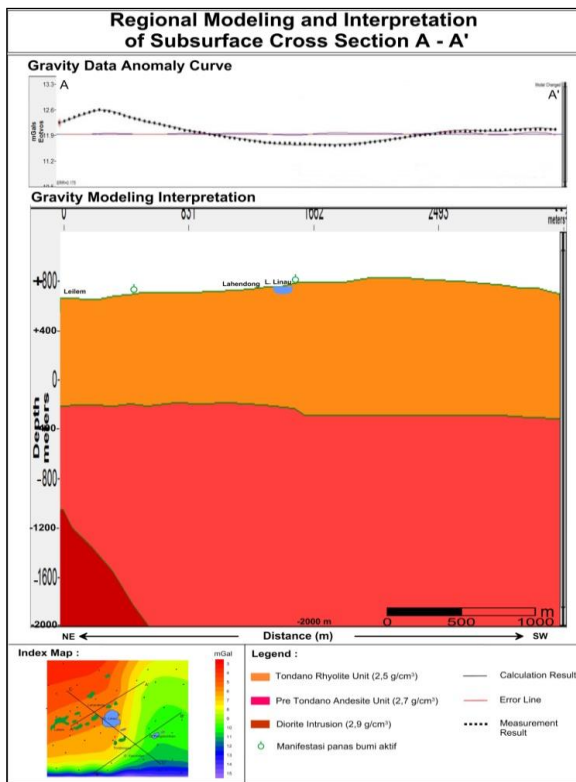


Fig 13. Regional modeling and interpretation of subsurface cross section A-A'

1) Cross Section A - A'

The results of regional gravity modeling cross section A – A' (Figure 13) show geological conditions below the deep surface with depths ranging from 800 m to (–2000) m. The results of regional (inside) gravity modeling and interpretation prove that there are 3 (three) rock layers along with rock density values, namely rock layers with a density value of (2,5 g/cm³) estimated became the Tondano Rhyolite Unit, rock layers with a density value of (2,7 g/cm³) is estimated became the Pre-Tondano Andesite Unit and the rock layer with a density value (2,9 g/cm³) is estimated became a diorite intrusion. There is a Diorite Intrusion layer reaching (-1000) m to (-2000) m which breaks through the Pre-Tondano Andesite Unit which is located in the NE direction of cross section A – A'.

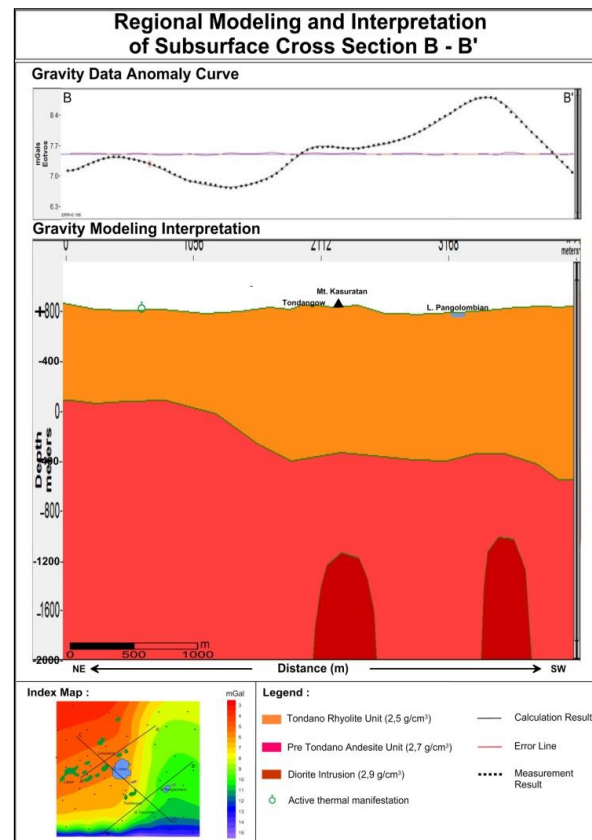


Fig 14. Regional modeling and interpretation of subsurface cross section B-B'

2) Cross Section B - B'

The results of regional gravity modeling cross section B – B' (Figure 14) show geological conditions below the deep surface with depths ranging from 800 m to (–2000) m. The results of regional (inside) gravity modeling and interpretation prove that there are 3 (three) rock layers along with rock density values, namely rock layers with a density value of (2,5 g/cm³) estimated became Tondano Rhyolite Unit, rock layers with a density value of (2,7 g/cm³) is estimated became Pre-Tondano Andesite Unit and the rock layer with a density value (2,9 g/cm³) is estimated became a diorite intrusion. The results of this modeling indicate that there are 2 (two) layers of Diorite Intrusion that break through Pre-Tondano Andesite Unit layer reaching a depth of (-1200) m to (-1000) m respectively. The presence of Diorite Intrusion layers is located at cross-sectional distances (2000 – 2300) m and (3400 – 3600) m.

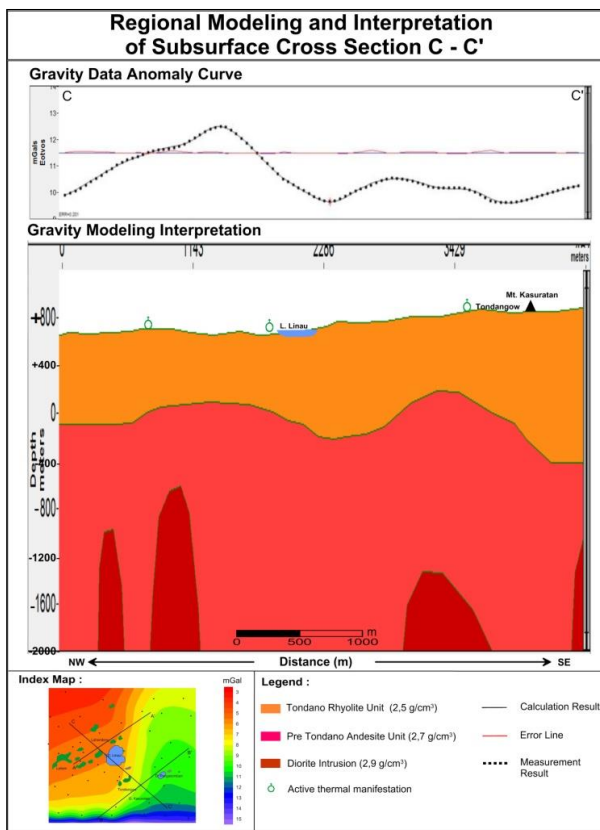


Fig 15. Regional modeling and interpretation of subsurface cross section C-C'

3) Cross Section C - C'

The results of regional gravity modeling cross section C – C' (Figure 15) show geological conditions below the deep surface with depths ranging from 800 m to (–2000) m. The results of regional (inside) gravity modeling and interpretation prove that there are 3 (three) rock layers along with rock density values, namely rock layers with a density value of (2.5 g/cm³) estimated became Tondano Rhyolite Unit, rock layers with a density value of (2.7 g/cm³) is estimated became Pre-Tondano Andesite Unit and rock layer with a density value (2.9 g/cm³) is estimated became a diorite intrusion. The results of this modeling indicate that there are 4 (four) layers of Diorite Intrusion that penetrate each other in Pre-Tondano Andesite Unit layer. The presence of the Diorite Intrusion layer is located at a cross-sectional distance of (300 – 400) m reaching a depth of (–1000 m) to (–2000) m, at a cross-sectional distance of (750 – 1100) m reaching a depth of (–600 m) to (–2000) m, at a cross-sectional distance (2900 – 3600) m reaching a depth of (–1400 m) to (–2000) m and at a cross-sectional distance of (4100 – 4200) m reaching a depth of (–1100 m) to (–2000) m.

6. Conclusion

The results of gravity modeling are composed of 4 rock layers, Post-Tondano Andesite Unit (2,0 gr/cm³), Tondano Rhyolite Unit (2,4 gr/cm³), Pre-Tondano Andesite Unit (2,6 gr/cm³) and diorite intrusion (2,9 gr/cm³). The interpretation of the geothermal system components in the “X” geothermal field consists of diorite intrusion suspected became heat source, and the Post-Tondano Andesite Unit suspected became reservoir rock. The Tondano Rhyolite Unit is thought became cap rock. The Pre-Tondano Andesite Unit is thought became the overburden. The existence of several normal fault structures becomes structure that controls the rise of hot fluid from the reservoir to the surface (manifestation).

Acknowledgments

Thanks to PT. Pertamina Geothermal Energy, especially the function of geophysics – resource management which has assisted and provided gravity data for the research area.

References

- Alsadi, H.N. & Baban, E.N. (2014). Introduction To Gravity Exploration Method. *Sulaimaniyah : First Edition*, Kurdistan Region, Iraq.
- Brehme, M., Moeck, I., Kamah, Y., Zimmermann, G., & Sauter, M. (2014). A Hydrotectonic Model of A Geothermal Reservoir – A Study In Lahendong, Indonesia, *Geothermics*, 51 (2014), p. 228–239.
- Brehme, M., Deon, F., Haase, C., Wiegand, B., Kamah, Y., Sauter, M. & Regenspurg, S. (2016). Fault controlled geochemical properties in Lahendong geothermal reservoir Indonesia. *Springer-Verlag Berlin Heidelberg, Grundwasser – Zeitschrift der Fachsektion Hydrogeologie* (2016) 21:29–41. DOI 10.1007/s00767-015-0313-9.
- Balmino, G. & Bonvalot, S. (2016). Gravity Anomalies. *Springer International Publishing Switzerland*, E.W. Grafarend (ed.), Encyclopedia of Geodesy, DOI 10.1007/978-3-319-02370-0_45-1.
- Dentith, M. & Mudge, S.T. (2014). *Geophysics for the Mineral Exploration Geoscientist*. Cambridge University Press.
- Fanani, A.F., Prabowo, T., Hastriansyah, G., Pasaribu, F. & Silaban, M. (2021). Application of the Flow Production Test to Update Well Production Capacity in Lahendong Geothermal Field. *Proceedings World Geothermal Congress*, Reykjavik, Iceland, April - October 2021.
- Gregg, A., Nordquist, Jorge, A. & Stimac, J. (2010). Precision Gravity Modeling and Interpretation at the Salak Geothermal Field, Indonesia. *Proceedings World Geothermal Congress 2010*, Bali, Indonesia, 25-29 April 2010.
- Hirt, C. (2015). Gravity forward modelling. *In: Encyclopaedia of Geodesy* (Ed. E. Grafarend).
- Ibrahim, M. M., Utami, P., & Raharjo, I. B. (2022). Analisis Struktur Geologi Berdasarkan Data Gravitasi Menggunakan Metode Second Vertical Derivative (SVD) Pada Lapangan Panas Bumi ”X”. *Jurnal Geosains dan Remote Sensing (JGRS)*, Vol 3, No 2 (2022) 52-59.
- Kristiawan, Y., Adityarani, M., Prasetyo, F.X.C., Naafiyanto, D.R., Harijoko, A., & Utami, P. (2013). Penerapan Studi Vulkanologi Dalam Penyelidikan Panas Bumi: Studi Kasus Pada Beberapa Lapangan Panas Bumi Di Indonesia, *Proceedings, 13th Indonesia International Geothermal Convention & Exhibition 2013*, Assembly Hall - Jakarta Convention Center Indonesia, June 12 – 14, 2013.
- LaFehr, T.R. (1991). *An Exact Solution for the Gravity Curvature (Bullard B) Correction*. *Geophysics* Vol. 56, No. 8, P. 1179-1184.
- Lestari, I. dan Sarkowi, M., 2013, Analisis Struktur Patahan Daerah Panasbumi Lahendong - Tompaso Sulawesi Utara Berdasarkan Data Second Vertical Derivative (SVD) Anomali Gayabarat, *Seminar Nasional Sains & Teknologi V*, Lembaga Penelitian Universitas Lampung 19-20 November 2013.
- PT. Pertamina Upstream Technology Center (2013). Studi Evolusi Pusat Aliran Panas dan Fluida Magmatik Sistem Panas Bumi Lahendong Untuk Pembuatan Rencana Pengembangan Lapangan. *Project Report for Pertamina Upstream Technology Center*, UGM Faculty of Engineering. Contract No. 47/D30140/2013-SO, (Unpublished).
- Sumintadireja, P., Ushijima K., & Sudarman, S. (2000). Misealarnasse and Gravity Data Surveys at The Kamojang Geothermal Field. *Proceeding World Geothermal Congress 2000*, Japan. P 1784.

- Sarkowi, M. (2014). *Gravity Exploration*. Yogyakarta, Indonesia: Graha Ilmu.
- Sidqi, M. & Utami, P. (2018). The Geology and Geothermal Systems of The Minahasa District, North Sulawesi, *Proceedings, The 6th Indonesia International Geothermal Convention & Exhibition (IIGCE) 2018*, Cendrawasih Hall - Jakarta Convention Center Indonesia, September 5th - 8th, 2018.
- Telford, W.M., Geldart, L.P. & Sheriff, R.E. (1990). *Applied Geophysics*, Second Edition edn, Vol., pp. Pages, Cambridge University Press, Cambridge.
- Utami, P. (2011). *Hydrothermal Alteration and The Evolution of The Lahendong Geothermal System, North Sulawesi, Indonesia*. A thesis submitted in fulfillment of the requirements for the degree of Doctor of Philosophy in Geology, The University of Auckland.
- Utami, P., Widarto, D.S., Atmojo, J.P. Kamah, Y., Browne, P.R.L., Warmada, I. W., Bignall, G. & Chambeft, I. (2015). Hydrothermal Alteration and Evolution of the Lahendong Geothermal System, North Sulawesi. *Proceedings World Geothermal Congress*, Melbourne, Australia.
- Utami, P., Sidqi, M., Siahaan, Y., Shalihin, M.G.J., Siahaan, E.E. & Silaban, M. (2021). Geothermal Prospects in Lahendong Geothermal Field of the Tomohon – Minahasa Volcanic Terrain (TMVT), North Sulawesi, Indonesia. *Proceedings World Geothermal Congress*, Reykjavik, Iceland, April - October 2021.



© 2024 Journal of Geoscience, Engineering, Environment and Technology. All rights reserved. This is an open access article distributed under the terms of the CC BY-SA License (<http://creativecommons.org/licenses/by-sa/4.0/>).